# Spectroscopic Studies of Bacteriorhodopsin Fragments Dissolved in Organic Solution

Jaume Torres and Esteve Padrós
Unitat de Biofísica, Departament de Bioquímica i de Biologia Molecular, Facultat de Medicina, Universitat Autònoma de Barcelona, Barcelona, Spain

ABSTRACT Fourier transform infrared and UV fourth-derivative spectroscopies were used to study the secondary structure of bacteriorhodopsin and its chymotryptic and one of the sodium borohydride fragments dissolved in chloroform-methanol (1:1, v/v), 0.1 M $LiClO_4$. The C1 fragment (helices C, D, E, F, and G) showed an $\alpha$-helical content of about 53%, whereas C2 (helices A and B) had about 60%, and B2 (helices F and G) about 65% $\alpha$-helix. The infrared main band indicated differences in $\alpha$-helical properties between these fragments. These techniques were also used to obtain information on the interactions among helices. According to the results obtained from the hydrogen/deuterium exchange kinetics, about 40% of the amide protons of C2 are particularly protected against exchange, whereas for the C1 fragment this process is unexpectedly fast. UV fourth-derivative spectra of these samples were used to obtain information about the environment of Trp side chains. The results showed that the Trp residues of C2 are more shielded from the solvent than those of C1 or B2. The results of this work indicate that the specific interactions existing between the transmembrane segments induce different types of helical conformations in native bacteriorhodopsin.

## INTRODUCTION

Bacteriorhodopsin (BR), the sole protein of *Halobacterium salinarium* purple membrane (PM), is one of the best characterized membrane proteins (for recent reviews see Rothschild, 1992; Oesterhelt et al., 1992; Ebrey, 1993). BR is organized into trimers that form two-dimensional hexagonal crystalline patches within the cell membrane. A near-atomic model of BR has been established using electron diffraction (Henderson et al., 1990), which unambiguously shows that BR consists of seven transmembrane $\alpha$-helices. The retinal molecule, which gives the characteristic purple color to the membrane, is linked to the protein via a protonated Schiff base to Lys-216. Because of the very low mobility of amino acids in membrane proteins, the nuclear magnetic resonance (NMR) technique has been to date only of limited application in elucidating the structure of BR (Seigneuret et al., 1991; Tuzi et al., 1993).

An alternative approach can be the study of BR conformation in a membrane-mimicking solvent. Arseniev et al. (1987) showed by CD spectroscopy and $^{19}$F-NMR that BR solubilized in organic solvents could have a secondary and tertiary structure quite similar to the native state. Following that work, conformational analysis of several synthetic fragments, e.g., B (Arseniev et al., 1988), A (Pervushin and Arseniev, 1992), and proteolytic fragments BP2 (Barsukov et al., 1990) and C2 (Sobol et al., 1992) by 2D $^1$H-NMR have been carried out. These works show the existence of a predominant structure, a right-handed $\alpha$-helix that fits well with the transmembrane segments obtained by electron cryomicroscopy (Henderson et al., 1990).

For infrared studies, this solvent not only eliminates the problem of subtracting the aqueous buffer contribution, but also permits the BR fragments to be studied separately. Furthermore, in spite of the absence of the charged interphase in this organic solvent, other integral membrane systems also show several native-like characteristics, as, e.g., subunit c of $F_1F_0$ ATP synthase from *Escherichia coli*. Not only are the two transmembrane $\alpha$-helices of this subunit present in the organic solvent, but they also retain precise conformational features (Fillingame et al., 1993). Thus, although the extrapolation of conformational characteristics of BR in this solvent to the native state remains to be established, it can nevertheless be used as a general indication of conformational trends.

In this work, we extend previous Fourier transform infrared (FTIR) results made on BR dissolved in chloroform/methanol mixture (Torres and Padrós, 1993). One of our goals is to try to differentiate between the BR $\alpha$-helices with respect to their conformational characteristics. We use fourth-derivative spectroscopy in the UV to monitor Trp residues environment, and FTIR to study secondary structures and also to obtain an indication of backbone shielding through hydrogen/deuterium exchange. These techniques are applied to whole BR as well as to the fragments obtained by chymotrypsin cleavage (C1: helices C–G, and C2: helices A and B) and one fragment obtained by $NaBH_4$ cleavage (B2: helices F and G).

## MATERIALS AND METHODS

### PM isolation

PM was isolated from *Halobacterium salinarium* strain S9 as described (Oesterhelt and Stoeckenius, 1974). The purity of the samples was checked by electrophoresis and UV-visible spectrophotometry.

*Received for publication 22 August 1994 and in final form 7 February 1995.*
Address reprint requests to Esteve Padrós, Unitat de Biofísica, Facultat de Medicina, Universitat Autònoma de Barcelona, 08193 Bellaterra, Barcelona, Spain. Tel.: 34-3-581-1870; Fax: 34-3-581-1907. E-mail: epadros@cc.uab.es

0006-3495/95/05/2049/07 $2.00

## Sodium borohydride cleavage

PM (2 mg/ml in water) was diluted with an equal volume of 6% w/v sodium borohydride, 0.1 M sodium carbonate, pH 10. The mixture was allowed to react at 4°C in the dark for 2 days under gentle stirring. The reaction was stopped by the addition of 5 volumes of 0.1 M sodium phosphate buffer (pH 6.0). The sample was washed twice with distilled water and lyophilized. Electrophoretic controls showed that about 40% of the protein was cleaved.

## Chymotryptic cleavage

Chymotryptic fragments were prepared as described by Popot et al. (1987). PMs (2 mg/ml) in 4 M NaCl, 1 M $NH_2OH$ (pH 7.5), were irradiated at room temperature with a 150-W lamp through a Wratten filter (520 nm high pass cutoff). After 12 h the sample was washed three times with distilled water (40,000 × *g*, 30 min). Apomembranes (2 mg/ml) were supplemented with Tris.HCl and $CaCl_2$ (final concentrations 50 and 5 mM, respectively; pH 8.0) and Nα-*p*-tosyl-L-lysine chloromethyl ketone-treated chymotrypsin (1 g/60 g BR), and incubated for 3.5 h at 37°C. Proteolysis was terminated by cooling to 4°C, and the sample was washed three times (40,000 × *g*, 45 min) with distilled water and lyophilized.

## Purification of the fragments

Chymotryptic or sodium borohydride fragments were separated on a Sephadex LH-60 column (2.5 × 90 cm) in chloroform/methanol (C/M), (1:1 v/v), 0.1 M $LiClO_4$. (When chymotryptic fragments or BR were passed through LH60 in formic acid/ethanol, and the dried aliquots solubilized in C/M, the solubility was poor and in the order C2>C1>BR. In the infrared, the amide I width was very large indicating the existence of broad absorption bands probably due to highly randomized structures. When these samples were solubilized after LH60 C/M chromatography the solubility was very high, suggesting that the protein was in a compact conformation so as to allow the interaction of solvent with residues involved in lipid interaction in the native state.) The corresponding fraction was evaporated and, after salt removal by centrifugation in $H_2O$, dried. Infrared (IR) samples were prepared by solubilizing the lyophilizate in the C/M mixture. The samples were vortexed and centrifuged at 12,000 × *g* for 5 min to remove unsolubilized material.

## UV fourth-derivative spectrophotometry

UV spectra were obtained on a Perkin-Elmer (Perkin-Elmer Co., Norwalk, CT) model 320 spectrophotometer in the range 340–260 nm with a resolution of 0.1 nm. The scan speed was 10 nm/min. In all cases, 10 scans were collected and averaged to improve the signal-to-noise (SN) ratio. Fourth-derivative spectra were calculated using the algorithm of Savitzki and Golay (1964).

## IR spectroscopy

Infrared spectra were acquired on a Mattson Polaris (Mattson Co., Madison, WI) FTIR spectrometer equipped with a Mercury-Cadmium-Telluride detector, working at an instrumental resolution of 2 $cm^{-1}$. Unless otherwise stated, for each sample 500 scans were averaged using a sample shuttle, apodized with a triangle function, and Fourier transformed. Absorbance spectra were obtained by digital subtraction of solvent spectra recorded under identical conditions. The spectrometer was continuously purged with dry air (dew point <−60°C). The sample temperature was kept at 20°C. Samples were placed in 50 μm pathlength IR cells and fitted with Teflon spacers between two $CaF_2$ windows.

Fourier deconvolution was performed using a full width at half height (FWHH) of 15 $cm^{-1}$, and the narrowing factor *k* was selected depending on the signal-to-noise (SN) ratio. Typically a value of 3 was used. In all cases, it was well below log(*SN*) (Kaupinnen et al., 1981).

## Hydrogen/deuterium exchange

The lyophilized samples were resuspended in deuterated chloroform/methanol (1:1, v/v), 0.1 M $LiClO_4$. This was taken as $t = 0$ in the kinetic study. After solubilization and centrifugation, the clear supernatant was used to obtain IR spectra at different times to calculate the H/D exchange rate. The H/D exchange was calculated according to the formula:

$$\%\text{Unexchanged}(t) = \frac{\frac{A_{II}}{A_I}(t) - \frac{A_{II}}{A_I}(t_f)}{\frac{A_{II}}{A_I}(t_0) - \frac{A_{II}}{A_I}(t_f)} \times 100 \quad (1)$$

where $A_I$ and $A_{II}$ are the integrated areas of amide I and amide II. $A(t_0)$ is the integrated area of the amide when the sample is dissolved in non-deuterated solvent, and $A(t_f)$ is the integrated area of the amide in deuterated solvent after 2 weeks.

The integrated areas were calculated by curve-fitting the amide shape with lorentzian bands to account for baseline effects. The spectra at different times were deconvoluted to observe the behavior of individual bands through H/D exchange. We found that the parameters selected (FWHH = 15 $cm^{-1}$ and $k = 3$) were not critical for our purposes, and the process could be analyzed for a wide range of FWHH and *k* values.

# RESULTS

## Fourth-derivative spectrophotometry

The tryptophan environment in proteins can be analyzed using UV spectroscopy by monitoring the wavelength of the first minimum ($\lambda_1$; see Fig. 1) in the fourth-derivative spectrum as shown by Duñach et al. (1983). According to these authors, the position of this minimum decreases as the polarity of the solvent increases. A value of $\lambda_1$ near 292 nm would indicate a Trp in an aqueous environment, and a value of 293 nm or greater would be typical of a Trp in a non-aqueous environment. This method was used in the present work to compare the Trp environment of three BR fragments in C/M. The model used for Trp residues exposed to this solvent was NAcTrpamide, which shows a $\lambda_1$ value at 294.1 nm (Table 1). The same value was obtained for the B2 fragment, indicating that both Trp residues on helix F were facing the solvent. In the case of BR or C1 fragment, this value

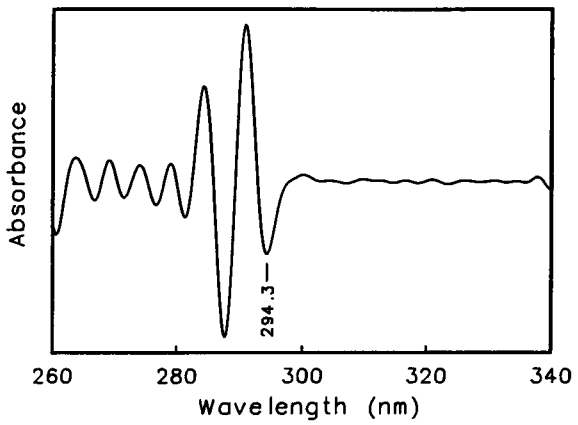


FIGURE 1 UV fourth-derivative spectrum of BR in C/M at 20°C. BR concentration, 1 × $10^{-5}$ M.

**TABLE 1 Values of $\lambda_1$ obtained from fourth-derivative UV spectra of bacteriorhodopsin and its fragments**

| Sample | Wavelength (nm) |
|---|---|
| PM in water | 294.3 |
| Bacteriorhodopsin in C/M | 294.3 |
| C1 in C/M | 294.3 |
| C2 in C/M | 294.5 |
| B2 in C/M | 294.1 |
| *N*-AcTrpamide in C/M | 294.1 |

increased to 294.3 nm, the same as obtained for PM suspended in water. As in this case eight and six Trp residues were involved; the value of $\lambda_1$ provides an estimation of the average environment of these residues and leads to some conclusions about the interactions between the helices in this solvent. First, the value obtained for both BR and C1 in C/M indicates that not all the Trp residues were facing the solvent, suggesting the presence of interactions between the helical rods. Secondly, the fact that this average value is the same indicates that the interactions present in BR among helices C–G were preserved after removal of the fragment C2. The value obtained for C2 also suggests that there existed some interactions between helices A and B, thus burying at least one of the two Trp residues of helix A in a relatively more hydrophobic environment. As shown in Fig. 2, the data obtained for fragments C2 and B2 are in accordance with the model proposed by Henderson et al. (1990) for native BR.

## Infrared spectra in chloroform/methanol

As has been previously indicated (Torres and Padrós, 1993) BR solubilized in C/M shows an amide I band centered at about 1653 $cm^{-1}$, whereas the intensity of the amide II band decreases to about one-half as compared with the native form (Fig. 3 *A*). The deconvoluted spectrum shows that the band centered at 1665 $cm^{-1}$ corresponding to $\alpha_{II}$-helix observed in the native PM is greatly decreased in this solvent, whereas other regions of amide I also show changes (Fig. 3 *B*). On the other hand, the absence of the 1742 $cm^{-1}$ band in the C/M sample indicates deprotonation of the Asp and Glu residues in the organic solvent, which should have a high apparent pH. Fig. 4 shows the deconvoluted amide I spectra corresponding to BR and fragments C1, C2, and B2 solubilized in C/M. As in BR, the 1665 $cm^{-1}$ band corresponding to $\alpha_{II}$ helices is

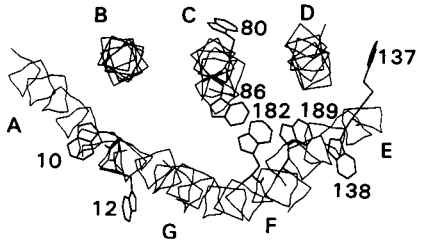


FIGURE 2 A backbone trace of the seven helices of BR, showing the location of Trp side chains. The coordinates were kindly provided by Dr. R. Henderson.

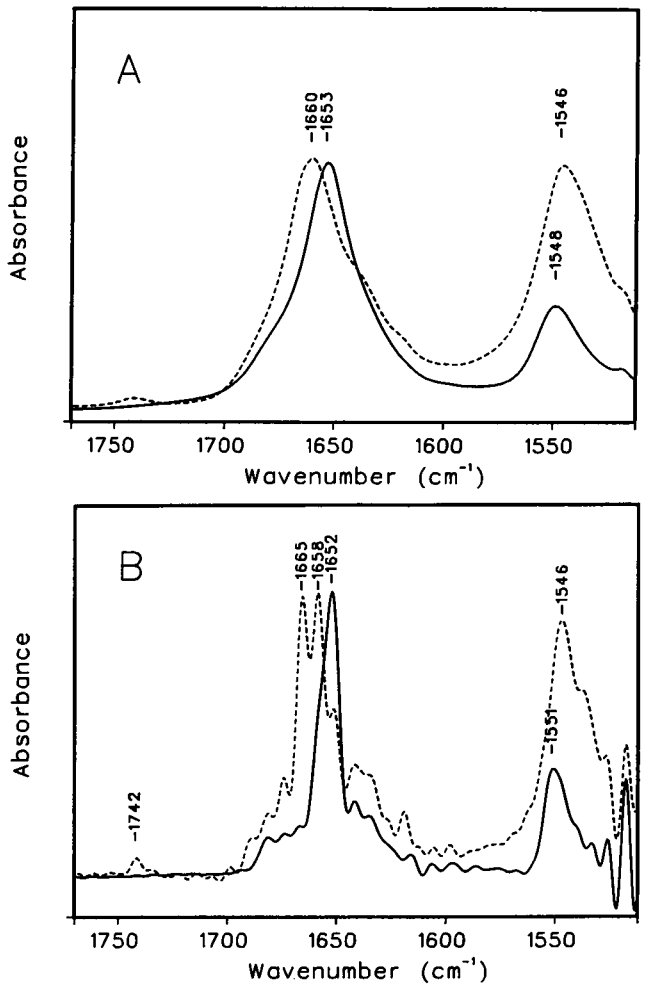


FIGURE 3 Absorption (*A*) and deconvoluted (*B*) spectra corresponding to PM in water, pH 6.0 (- - - - -) and to BR in C/M (———) in the amide region, at 20°C. BR concentration, $10^{-3}$ M; instrumental resolution, 2 $cm^{-1}$. The absorption spectra were obtained by co-adding 500 scans in blocks of 20 of the shuttle accessory. This helps to minimize the water vapor bands by compensating the small variations in water vapor concentration that could occur during the scanning. Deconvolutions were done using a bandwidth of 15 $cm^{-1}$ and a *k* factor of 3.

greatly decreased in the fragments, and the shoulder at about 1657 $cm^{-1}$ shows different intensity depending on the sample. In B2 the maximum is located at 1653 $cm^{-1}$, and the shoulder is poorly resolved. It cannot be detected in C2, in which case there is only one band at 1654 $cm^{-1}$. As the IR spectrum of C2 had an SN ratio better than 5000, the parameter *k* could be raised to 3.7 (Kauppinen et al., 1981) to increase the resolution of the deconvoluted spectrum. Despite the fact that the noise due to deconvolution is high at this *k* value, the expected two bands could not be detected by this procedure (not shown). The C1 fragment showed a maximum at 1651 $cm^{-1}$, similar to whole BR, with a visible shoulder. Quantification of the secondary structure content by curve-fitting the spectra showed that $\alpha$-helix is the predominant structure, giving the approximate values of 53% for C1, 60% for C2, and 65% for B2, as compared with about 70% for whole BR in C/M.

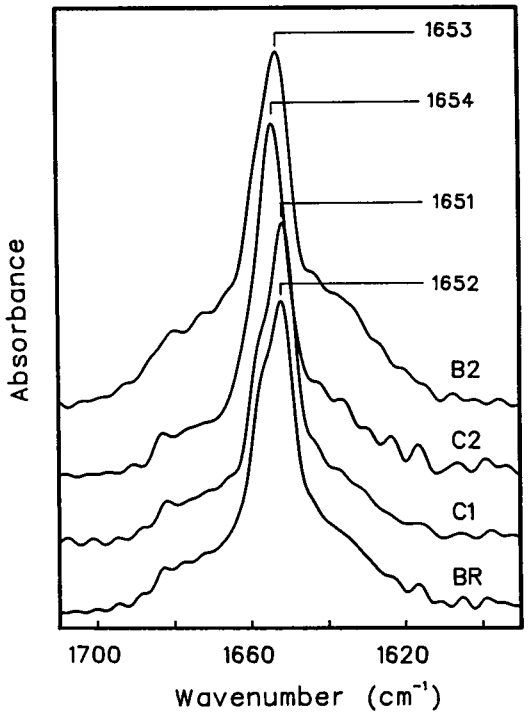


FIGURE 4 Deconvoluted amide I spectra corresponding to BR and fragments C1, C2, and B2, dissolved in C/M, at 20°C. Fourier deconvolutions were done using a bandwidth of 15 $cm^{-1}$ and a resolution enhancement factor of 2.7.

## Hydrogen/deuterium exchange of BR, C1, and C2

To obtain information about the secondary structure accessibility in chloroform/methanol, we studied the exchange rate of protons by deuterons by resuspending the lyophilized samples in deuterated solvent. As shown in Fig. 5, the exchange rate depends on the sample analyzed. For all the samples the percentage of unexchanged protons decreased exponentially with time. All the amide protons of C1 were exchanged after about 30 h, whereas for C2 it remained about 40% unexchanged by this time. The curve of BR corresponds to the sum of the last two curves, as expected. It was ascertained that a possible aggregation is not responsible for the behavior of the C2 fragment, as an exchange curve obtained at a lower concentration showed similar results (data not shown). The data corresponding to the fragment C2 are consistent with the NMR results obtained under identical conditions by Sobol et al. (1992), who reported that about 34% of the amide protons have exchange half-time between 10 and 100 h and the remaining ones less than 30 min.

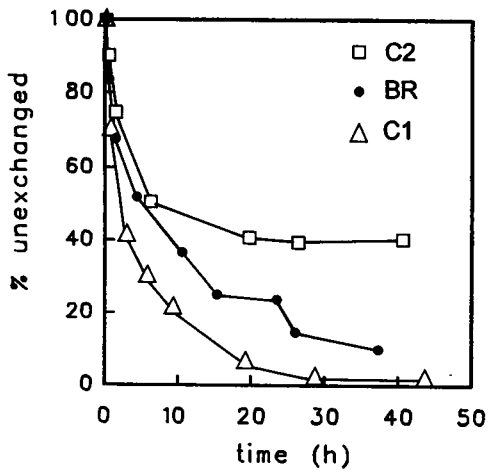


FIGURE 5 Plot of the percentage of unexchanged amide protons as a function of time after dissolution in the deuterated organic solvent for BR ($2 \times 10^{-4}$ M), C1 ($2 \times 10^{-4}$ M), and C2 ($4 \times 10^{-3}$ M).

The differences in the exchange rates of C1 and C2 should be reflected in the deconvoluted spectra taken at different times after addition of deuterated C/M. Also, this procedure can be used to separate bands that are too overlapped to be seen after deconvolution of the samples in non-deuterated C/M. In C1, a main band at 1651 $cm^{-1}$ and a shoulder at 1657 $cm^{-1}$ can be observed in the non-deuterated C/M sample (Fig. 6 *A*). As exchange proceeds, the band at 1657 $cm^{-1}$ shifts to 1655 $cm^{-1}$, and the 1652 $cm^{-1}$ band shifts to 1645 $cm^{-1}$. As the band at 1652 $cm^{-1}$ shifts to lower wavenumbers, the shoulder becomes more evident. After 2 days, by which time the exchange is complete, the shoulder is clearly resolved by deconvolution, giving a band centered at 1655 $cm^{-1}$. The results for the C2 fragment show that after 15 min of exchange, the single band at 1654 $cm^{-1}$ has split into two new bands centered at 1655 and 1652 $cm^{-1}$ (Fig. 6 *B*). This splitting into two bands could be due to a band centered between the other two that has exchanged very fast, probably a non-ordered structure. As can be seen in Fig. 6 *B*, the exchange is not complete after 2 days, showing two main bands at 1656 and 1649 $cm^{-1}$. These two bands shift slowly to lower wavenumbers, and after 2 weeks the exchange is complete (bands at 1655 and 1646 $cm^{-1}$). Therefore, for all the fragments analyzed, as well as for BR, we can observe two intense bands in the deconvoluted amide I region. These bands are assigned to helical structure, as their frequencies are within the range normally accepted for these structures (1650–1657 $cm^{-1}$; Byler and Susi, 1986; Surewicz and Mantsch, 1988). Furthermore, the sum of their relative areas is comparable to the predicted $\alpha$-helical content in this solvent (Arseniev et al., 1988; Pervushin and Arseniev, 1992; Sobol et al., 1992).

## DISCUSSION

In accordance with the model of Henderson et al. (1990) there are some Trp residues facing the lipids and some others facing the other helices (Fig. 2). When organic solvent is substituted for the lipids, the contribution of the outside Trp should imply a smaller $\lambda_1$ because of the increased polarity of C/M as compared with the lipids. The fact that $\lambda_1$ remains the same (Table 1) could be due to rearrangements of the interhelical interactions leading the inner Trp to more hydrophobic environments. Whatever the reason, it is important to point out that $\lambda_1$ is the same for both C1 and BR in this solvent, and this value does not correspond to the value obtained for NAcTRPamide. This supports the idea that in ad-

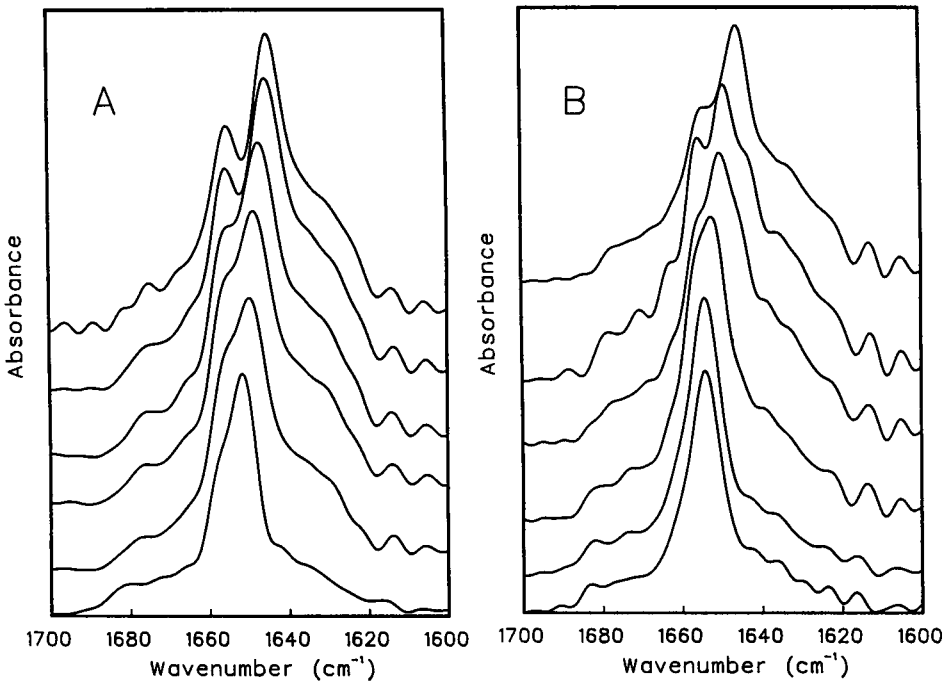


FIGURE 6 Deconvoluted amide I spectra of fragments C1 (*A*) and C2 (*B*) in deuterated C/M at 20°C, corresponding to the following times after addition of deuterated solvent to lyophilized samples (from bottom to top): 0 min, 0.5 h, 1.5 h, 5.5 h, 2 days, and 2 weeks.

dition to the similar trends found in the secondary structure, in the organic solvent there exists a defined three-dimensional disposition between the helical rods because of interhelical interactions. Our work clearly shows that about 40% of the amide protons in C2 remain unexchanged after 30 h at 20°C, whereas for C1 nearly all have been exchanged by this time. On the other hand, in BR about 10% of the amide protons exchange at a very low rate. This percentage fits the 40% of slow exchange amide protons in the C2 fragment, and this suggests that the time course in any of the fragments is not influenced by the presence of the complementary one. That is, the interactions of helices A and B with the other helices do not have any influence on the hydrogen bonds formed by the C1 amide protons. Therefore, the interactions between the helices corresponding to the two fragments in this solvent appear to be weak.

The recent finding that the calculated interaction energies of helices A and B are not influenced by the orientations of the other helices (Tuffery et al., 1994) gives additional support to the conformational similarities in terms of three-dimensional disposition of the seven helical rods in the native state and in this solvent. It is worth mentioning that the differences observed in the exchange rate for the two fragments could be attributed to an increased tendency of the C2 fragment to aggregate in the C/M solvent, thus decreasing the accessibility of some amide protons to the medium. However, this possibility can be excluded because the interactions between helices from different C2 fragments in this solvent have not been detected by NMR (Sobol et al., 1992). On the other hand, if the interaction between helices from the same fragment made some amide protons belonging to interacting faces inaccessible to the solvent, this fact should be reflected in NMR data, but it is clear that the exchange resistance does not depend on the face in which the residue is located (Sobol et al., 1992). Furthermore, the rate of exchange of individual helical rods in this solvent is similar to that found in the fragment C2 (A. Sobol, personal communication). Hence, the differences observed between fragments C1 and C2 from the point of view of H/D exchange in the organic solvent seem to be due to a different strength in the hydrogen bonds between amide protons and carbonyl groups within the helices. Also, the position of the amide I maxima among the three fragments (1651 $cm^{-1}$ for C1, 1653 $cm^{-1}$ for B2, and 1654 $cm^{-1}$ for C2) should reflect slight variations among the helices and can be ascribed to differences in hydrogen bonding.

This distinct behavior of helices A and B as compared with the rest could be related to general trends in amino acid composition. As indicated by Tuffery et al. (1994), helices A and B (and D) do not have a clear amphipathy, due to the almost complete lack of hydrophilic residues. The above results seem to agree with recent NMR studies made on BR in C/M solution (Orekhov et al., 1992). These authors explain the band broadening in the $^1H$–$^{15}N$ NMR spectra suggesting a conformational mobility that could lead to a weakening in the strength of the CO···HN bonds. Interestingly, they show specific interactions between rods corresponding to helices C, D, E, and F. According to these authors, one reason for such effects in these hydrogen bonds might be either a bending of the helical rods or the interconversion $\alpha_I/\alpha_{II}$ or both. Let us discuss this point in some detail. As it is known, the blue shift of IR amide I region of BR and the large splitting of the parallel and perpendicular modes of this band have led to the hypothesis of the existence of a significant number of $\alpha_{II}$-helices (Krimm and Dwivedi, 1982). Raman (Vogel and Gärtner, 1987), UV circular dichroism (Gibson and Cassim,

1989), far-UV CD, and mid-IR linear dichroism results (Draheim and Cassim, 1992) give support to the idea that about 50% of the BR helical-structure is $\alpha_{II}$-type. Although we do not detect in this solvent either $\alpha_{II}$ conformation or transition between $\alpha_I/\alpha_{II}$, we cannot exclude such transitions. Let us take into account the following assumptions: 1) there is an equilibrium between $\alpha_I$ and $\alpha_{II}$ conformations; 2) this equilibrium is shifted to $\alpha_I$, so we cannot detect $\alpha_{II}$; but 3) the equilibrium is fast enough to allow the small population of $\alpha_{II}$ to be in continuous turnover so that fast exchange in $\alpha_{II}$ could take place. Under these conditions, the equilibrium could be shifted toward one of the two conformations depending on the environment (Torres, Sepulcre, and Padrós, manuscript in preparation).

On the other hand, the different behavior in terms of stability of the fragments has already been reported. The results obtained by reconstitution in lipid/detergent-mixed micelles or in native lipid liposomes show that the C1 fragment, which contains the five C-terminal transmembrane segments of BR, denatures relatively rapidly in DMPC/Chaps/SDS ($t_{1/2} \approx 20$ min; Liao et al., 1983). Also, V2 fragment (helices F and G, obtained by protease V8 digestion) denatures with a $t_{1/2}$ of about 8 min, whereas denaturation of fragments C2 and V1 (helices A–E) is very slow, with a $t_{1/2}$ value of several hours (Sigrist et al., 1988). Whether this effect is due to a bending of the helical rods, transitions between $\alpha_I$ and $\alpha_{II}$ conformation, or both, the important fact is that the different strength in the CO···HN bonds corresponding to C1 and C2 fragments in C/M has been so far reported by two techniques. The existence of significant amounts of $\alpha_{II}$-helix in BR is still a subject of controversy as it cannot be resolved yet from $\alpha_I$ by diffraction methods. Nevertheless, the presence of different types of $\alpha$-helix in the transmembrane regions of native BR has been suggested using FTIR (Cladera et al., 1992), and more recently similar interpretations have been obtained using solid-state $^{13}$C-NMR (Tuzi et al., 1993). Although the origin of the amide I blue shift has been suggested to be due to the transition dipole moment coupling between localized vibrational modes in different $\alpha$-helices (Hunt, 1988; Hunt et al., 1988), the evidence presented in this work give supports to the existence of $\alpha_{II}$-helix in BR.

The authors thank Dr. Tzvetana Lazarova for critically reviewing the manuscript, Drs. Josep Cladera and Francesc Sepulcre for helpful discussions, and Dr. R. Henderson for sending us the BR coordinates. The excellent technical assistance of Elodia Serrano is gratefully acknowledged.

This work was supported by the Dirección General de Investigación Científica y Técnica (grant PB92–0622 to E.P. and fellowship to J.T.).

## REFERENCES

Arseniev, A. S., A. B. Kuryatov, V. I. Tsetlin, V. F. Bystrov, V. T. Ivanov, and Y. A. Ovchinnikov. 1987. $^{19}$F NMR study of 5-fluorotryptophan-labeled bacteriorhodopsin. *FEBS Lett.* 213:283–288.

Arseniev, A. S., I. V. Maslennikov, V. F. Bystrov, A. T. Kozhich, V. T. Ivanov, and Y. A. Ovchinnikov. 1988. Two-dimensional $^1$H-NMR study of bacterioopsin-(34–65)-polypeptide conformation. *FEBS Lett.* 231: 81–88.

Barsukov, I. L., G. V. Abdulaeva, A. S. Arseniev, and V. F. Bystrov. 1990. Sequence-specific $^1$H-NMR assignment and conformation of proteolytic fragment 163–231 of bacterioopsin. *Eur. J. Biochem.* 192: 321–327.

Byler, D. M., and H. Susi. 1986. Examination of the secondary structure of proteins by deconvolved FTIR spectra. *Biopolymers.* 25:469–487.

Cladera, J., M. Sabés, and E. Padrós. 1992. Fourier transform infrared analysis of bacteriorhodopsin secondary structure. *Biochemistry.* 31: 12363–12368.

Draheim, J. E., and J. Y. Cassim. 1992. Percent $\alpha$-II helix in bacteriorhodopsin. *Biophys. J.* 61:552*a* (Abstr.)

Duñach, M., M. Sabés, and E. Padrós. 1983. Fourth-derivative spectrophotometry analysis of tryptophan environment in proteins. Application to melittin, cytochrome *c* and bacteriorhodopsin. *Eur. J. Biochem.* 134: 123–128.

Ebrey, T. 1993. Light energy transduction in bacteriorhodopsin. *In* Thermodynamics of Membranes, Receptors and Channels. M. Jacobson, editor. CRC Press, Boca Raton, FL. 353–387.

Fillingame, R. H., M. E. Girvin, D. Fraga, and Y. Zhang. 1993. Correlations of structure and function in $H^+$ translocating subunit c of $F_1F_0$ ATP synthase. *Ann. N. Y. Acad. Sci.* 671:323–334.

Gibson, N. J., and J. Y. Cassim. 1989. Evidence for an $\alpha_{II}$-type helical conformation for bacteriorhodopsin in the purple membrane. *Biochemistry.* 28:2134–2139.

Henderson, R., J. M. Baldwin, T. A. Ceska, F. Zemlin, E. Beckmann, and K. H. Downing. 1990. Model for the structure of bacteriorhodopsin based on high-resolution electron cryo-microscopy. *J. Mol. Biol.* 213:899–929.

Hunt, J. F., T. N. Earnest, D. M. Engelman, and K. J. Rothschild. 1988. An FTIR study of integral membrane protein folding. *Biophys. J.* 53:97*a*. (Abstr.)

Hunt, J. F. 1988. An influence of tertiary structure on protein infrared spectra. *Biophys. J.* 53:97*a*. (Abstr.)

Kauppinen, J. K., D. J. Moffatt, H. H. Mantsch, and D. G. Cameron. 1981. Fourier self-deconvolution: A method for resolving intrinsically overlapped bands. *Appl. Spectrosc.* 35:271–276.

Krimm, S., and A. M. Dwivedi. 1982. Infrared spectrum of the purple membrane: clue to a proton conduction mechanism? *Science.* 216: 407–408.

Liao, M. J., E. London, and H. G. Khorana. 1983. Regeneration of the native bacteriorhodopsin structure from two chymotryptic fragments. *J. Biol. Chem.* 258:9949–9955.

Oesterhelt, D., and W. Stoeckenius. 1974. Isolation of the cell membrane of *Halobacterium halobium* and its fractionation into red and purple membrane. *Methods Enzymol.* 31:667–678.

Oesterhelt, D., J. Tittor, and E. Bamberg. 1992. A unifying concept for ion translocation in retinal proteins. *J. Bioenerg. Biomembr.* 24:181–191.

Orekhov, V. Y., G. V. Abdulaeva, L. Y. Musina, and A. S. Arseniev. 1992. $^1$H-$^{15}$N-NMR studies of bacteriorhodopsin *Halobacterium halobium*. Conformational dynamics of the four-helical bundle. *Eur. J. Biochem.* 210:223–229.

Pervushin, K. V., and A. S. Arseniev. 1992. Three-dimensional structure of (1–36)bacterioopsin in methanol-chloroform mixture and SDS micelles determined by 2D $^1$H-NMR spectroscopy. *FEBS Lett.* 308: 190–196.

Popot, J-L., S-E. Gerchman, and D. M. Engelman. 1987. Refolding of bacteriorhodopsin in lipid bilayers. A thermodynamically controlled two-stage process. *J. Mol. Biol.* 198:655–676.

Rothschild, K. 1992. FTIR difference spectroscopy of bacteriorhodopsin: toward a molecular model. *J. Bioenerg. Biomembr.* 24:147–167.

Savitzky, A., and M. J. Golay. 1964. Smoothing and differentiation of data by simplified least squares procedures. *J. Anal. Chem.* 36:1627–1639

Seigneuret, M., J. M. Neumann, and J. L. Rigaud. 1991. Detergent delipidation and solubilization strategies for high-resolution NMR of the membrane protein bacteriorhodopsin. *J. Biol. Chem.* 266: 10066–10069.

Sigrist, H., R. H. Wenger, E. Kislig, and M. Wüthrich. 1988. Refolding of bacteriorhodopsin. Protease V8 fragmentation and chromophore reconstitution from proteolytic V8 fragments. *Eur. J. Biochem.* 177:125

Sobol, A. G., A. S. Arseniev, G. V. Abdulaeva, L. Y. Musina, and V. F. Bystrov. 1992. Sequence-specific resonance assignment and secondary structure of (1–71) bacterioopsin. *J. Biomol. NMR.* 2:161–171.

Surewicz, W. K., and H. H. Mantsch. 1988. New insight into protein secondary structure from resolution-enhanced infrared spectra. *Biochim. Biophys. Acta.* 952:115–130.

Torres, J., and E. Padrós. 1993. The secondary structure of bacteriorhodopsin in organic solution. A Fourier transform infrared study. *FEBS Lett.* 318:77–79.

Tuffery, P., C. Etchebest, J.-L. Popot, and R. Lavery. 1994. Prediction of the positioning of the seven transmembrane α-helices of bacteriorhodopsin. A molecular simulation study. *J. Mol. Biol.* 236:1105–1122.

Tuzi, S., A. Naito, and H. Saito. 1993. A high-resolution solid-state $^{13}C$-NMR study on [1-$^{13}C$]Ala and [3-$^{13}C$]Ala and [1-$^{13}C$]Leu and Val-labelled bacteriorhodopsin. Conformation and dynamics of transmembrane helices, loops and termini, and hydration-induced conformational change. *Eur. J. Biochem.* 218:837–844.

Vogel, H., and W. Gärtner. 1987. The secondary structure of bacteriorhodopsin determined by Raman and Circular Dichroism spectroscopy. *J. Biol. Chem.* 262:11464–11469.